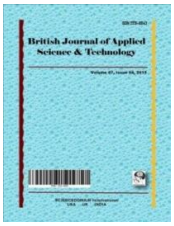

British Journal of Applied Science & Technology
17(1): 1-10, 2016, Article no.BJAST.28143
ISSN: 2231-0843, NLM ID: 101664541

SCIENCEDOMAIN *international*
www.sciencedomain.org

Characterizations of Beta-lead Oxide "Massicot" Nano-particles

Sarah A. Elawam[1], Wafaa M. Morsi[2], Hoda M. Abou-Shady[3] and Osiris W. Guirguis[1*]

[1]Department of Biophysics, Faculty of Science, Cairo University, Giza, Postcode: 12613, Egypt.
[2]Building Physics Institute, Housing and Building National Research Center (HBRC), Giza, Egypt.
[3]Department of Physics, Faculty of Science, Cairo University, Giza, Postcode: 12613, Egypt.

Authors' contributions

This work was carried out in collaboration between all authors. All authors read and approved the final manuscript.

Article Information

DOI: 10.9734/BJAST/2016/28143
Editor(s):
(1) João Miguel Dias, Habilitation in Department of Physics, CESAM, University of Aveiro, Portugal.
Reviewers:
(1) Matheus Poletto, Universidade de Caxias do Sul, Brazil.
(2) Yong Gan, California State Polytechnic University-Pomona, USA.
(3) Lexter R. Natividad, Central Luzon State University, Philippines.
Complete Peer review History: http://www.sciencedomain.org/review-history/15586

Original Research Article

Received 4th July 2016
Accepted 21st July 2016
Published 30th July 2016

ABSTRACT

The present work objective is to prepare and study beta-lead oxide (β-PbO) "massicot" nano-powders by sol-gel method. The lead oxide nano-powders were synthesized through the reaction of lead diacetate solution and oxalate solution. The thermal stability and characterization of the compound were investigated by thermogravimetric (TGA) and differential scanning calorimetry (DSC) analyses, X-ray powder diffraction (XRD) and Fourier transform infrared (FT-IR) techniques. The morphology and crystallographic structural forms were performed by scanning electron microscopy (SEM), high-resolution transmission electron microscopy (HRTEM) and selected area electron diffraction (SAED). The obtained TGA and DSC data indicate that the prepared PbO nano-particles are stable. The XRD, HRTEM and SAED data indicate that a mixture of Pb, litharge (tetragonal PbO), and massicot (orthorhombic PbO) were formed with average crystalline size of about 84 nm. The SAED pattern revealed that the formed nano-particles are β-PbO which it was dominant because the annealing temperature was above 400°C.

**Corresponding author: E-mail: osiris_wgr@yahoo.com;*

Keywords: Nano-particles; lead oxide; sol-gel method; thermal analyses; morphology and crystallographic structure; FT-IR.

1. INTRODUCTION

The chemical and physical properties of solid materials strongly depend on both the size and the shape of the microscopic particles they were made from. It is especially true for materials with morphological features smaller than a micron in at least one dimension, which was commonly called nano-scale materials, or simply nano-materials [1]. Due to the particular physical and chemical properties and also, the potential applications in various scientific and industrial fields, nano-materials have attracted the attention of many researchers [2,3]. In addition, nano-materials were used in gas sensors, fuel cells, paints, rechargeable batteries and pigments due to their small sizes. Furthermore, because nanostructures materials have a long axis to absorb incident sunlight, one-dimensional (1D) nanostructures have gained attention in solar energy conversion [4]. For example, Nandy et al. [5] studied the characterization of copper doped zinc oxide nano-particles and its application in energy conversion.

Lead oxides are fascinating compounds because of their numerous phases. These stages include four fundamental types; PbO (α, β and amorphous), Pb_2O_3, Pb_3O_4, PbO_2 (α, β and amorphous) [6,7,8]. PbO has two polymorphic forms and a wide band gap. One of these two forms is the yellow β-PbO, which is stable at temperatures higher than 425°C. The second form is the red α-PbO, which is stable at low temperature. The α-PbO phase transformation to β-PbO takes place at about 490°C [2,9]. However, the high-temperature yellow form can exist even at room temperature. PbO is transparent conducting oxide (TCO) that has a high dielectric constant (ε' = 525.9) [10]. It is also a high refractive index material. Both α-PbO and β-PbO are photoactive semiconductors with band gaps of 1.92 and 2.7 eV, respectively [6,11,12]. A mixture of α and β-PbO nano-crystals could be obtained via the calculation of both lead citrate and lead oxalate [13].

In recent years, attention on the synthesis of PbO nano-structures was increased due to its easy preparation as well as its electronic, mechanical and optical properties and also due to its potential applications in nano-devices and functionalized materials [7,11,14,15,16]. PbO nano-particles with its both shapes had been used in medical applications such as; gamma ray protective clothing, shielding, magnetic imagining, batteries, X-ray sensing application and in pharmaceutical applications such as drug delivery. The most recent studies demonstrated that the rod and spherical shaped nano-lead oxides have antibacterial uses. Also, PbO is amphoteric which means that it reacts easily with both acid and base [17].

Lead oxide nanostructure could be synthesized using various methods [7,18,19,20,21]. The sol–gel method shows considerable advantages over the customary methods and provides a low cost, simple, non-hazardous technique for the preparation of different nano-oxides. Kashani-Motlagh and Mahmoudabad [16] used the sol-gel method to synthesize and characterize lead oxide nano-powders.

On other hand, the necessity of more efficient radiation shielding and structural materials grows as the medical, pharmaceutical, nuclear and space industries require lighter, tougher, and higher radiation resistant materials. In this regard, various studies were performed recently [22,23,24,25]. To summarize the studies, lead monoxide (PbO) was successful in shielding radiation such as X-rays or γ-rays due to its high density (≈ 9.53 g/cm^3) [26].

In the present work, lead oxide nano-powders were prepared to be used in different applications. The sol-gel method was used due to its simple, inexpensive, and economical and was introduced as reproducible process for the large-scale synthesis of PbO nano-particles. Characterization of the prepared nano-particles has been made using X-ray diffractometry in addition to the particles morphology using the transmission electron microscope. To get more information about the synthesized particles, thermogravimetric analysis, differential scanning calorimetry and Fourier transform infrared spectroscopy were investigated.

2. EXPERIMENTAL DETAILS

2.1 Materials and Sample Preparation

In the present work, high purity lead diacetate of chemical formula [$Pb(CH_3COO)_2$] with average molecular weight of 279.33 and oxalic acid [$C_2H_2O_4$] of molecular weight 126.07, supplied from Adwik, Egypt, were used.

Lead oxide (PbO) nano-particles were synthesized via sol-gel method [27,28]. First, 75.868 g of lead diacetate and 18.008 g of oxalic acid oxalate were dissolved in 200 mL double distilled water (DD) under a magnetic stirring for about 1 hour at 60°C to mix all of the chemicals homogeneously until given a white colloidal suspension. The obtained sol was kept in an electrical oven for 8 hours at about 80°C, and then the temperature gradually decreases to room temperature (about 25°C) through 4 hours with keeping the suspension in the oven, and, so, stirred to obtain the gel form. The obtained gel was aged for 18 h at room temperature. The gel was calcined at a temperature of about 900°C for 1 hour, to obtain get yellow-greenish powders of lead oxide (β-PbO), i.e., "massicot".

2.2 Characterizations Techniques

The thermal analyses of the prepared nano-powders were studied by using Thermogravimetric Analyzer model Schimadzu TGA-50H (Kyoto, Japan) and Differential Scanning Calorimetry (DSC) model Schimadzu DSC-50 (Kyoto, Japan) cover the range from 25 to 650°C. TGA and DSC analyses were performed under nitrogen flow of 20 mL/minute at heating rate of 10°C/minute.

The X-ray diffraction (XRD) measurement of the prepared PbO nano-particles was recorded by using Phillips PW1840 X-Ray Diffractometer (USA) with an anode tube of CuK_{α} radiation (λ = 1.54056 Å), operated at 40 kV and 25 mA. The diffractogram was recorded in the range of 2θ from 5 to 70° at a speed rate of 2 degrees/ minute.

The surface morphology of PbO sample was analyzed by using the Scanning Electron Microscopy (SEM; Inspect S, FEI, Holland) at a low vacuum mode, after allowing it to spread on a small metal circular plate at operating voltage of 30 kV and a magnification power of 13000X. In the SEM an electron beam was focused into a fine probe and subsequently scanned over a small rectangular area. The beam interacts with the sample and creates various signals (secondary electrons, internal currents, photon emission, etc.). All these signals were detected.

High-Resolution Transmission Electron Microscopy (HRTEM; JEM 2100, Jeol, Japan) was used to reach high resolution and obtain bright field, and dark field images of the particles. These images were used to detect the outer surface and inner-structures of the particles and to test the crystalline size of the as-synthesized PbO nano-particles.

The Fourier Transform Infrared (FT-IR) transmission spectrum of the prepared PbO nano-particles was obtained using potassium the bromide pellet technique [29]. The pellets were prepared by mixing 1 mg of powdered sample with 100 mg of dried potassium bromide powders. The mixing was performed using a pestle and agate mortar. The mixture was then pressed in a special die at a pressure of 10,000 pounds per square inch to yield a disk. The pellets were measured before and after being kept in an oven at 400°C for 2 hours. The FT-IR spectrum was recorded at room temperature by using Perkin-Elmer FT-IR Spectrophotometer model 1650 TX in the wavenumber range from 4000 to 450 cm^{-1} with a resolution of 4 cm^{-1}.

3. RESULTS AND DISCUSSION

In order to examine the thermal stability of the PbO nano-sized particles, thermal gravimetric (TGA) and differential scanning calorimetry (DSC) were carried out between 25 and 650°C (Figs. 1 and 2, respectively). Fig. 1 show clearly that the prepared PbO nano-sized particles are very stable and do not decompose up to a temperature of about 225°C. At 225°C, the decomposition of the compound starts. Between this temperature and 500°C the decomposition occurs with a weight loss of 1.47% which may be attributed to the decomposition of lead oxalate to lead oxide. This occurs because the oxidation number of the lead ions is constant during the thermal decomposition process [2,16,30]. As a consequence, lead oxide forms at temperatures as low as 500°C.

From Fig. 2, the DSC curve shows that the prepared PbO nano-sized particles is stable up to 120°C at which temperature it loses the coordinated water molecules with an endothermic effect at about 123°C and heat enthalpy 0.193 J/g. In addition, the DSC curve for the prepared sample displays two distinct endothermic effects at about 245 and 332°C with heat enthalpy of 2.61 and 2.92 J/g, respectively. The onset at 320.7°C in the DSC analysis report of the sample is the melting point, which is in good agreement with the lead nano-particles synthesized by other methods.

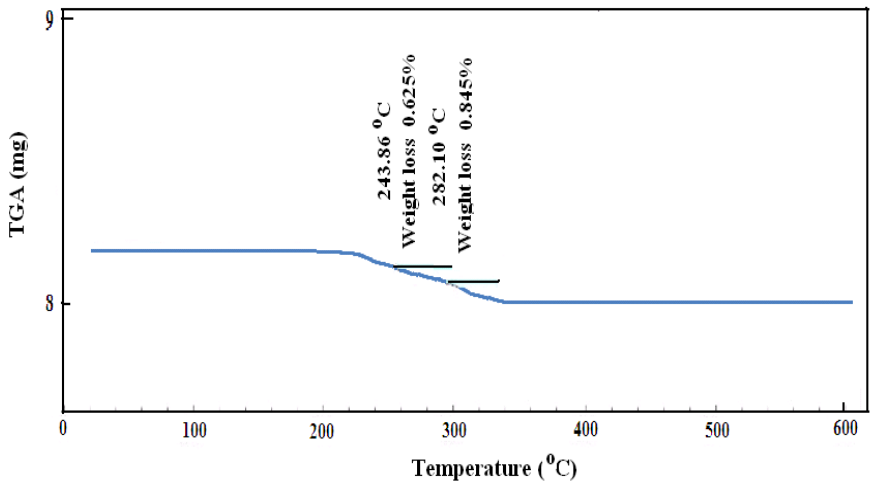

Fig. 1. TGA plot of the prepared lead oxide nano-particles associated with the decomposition at different temperatures

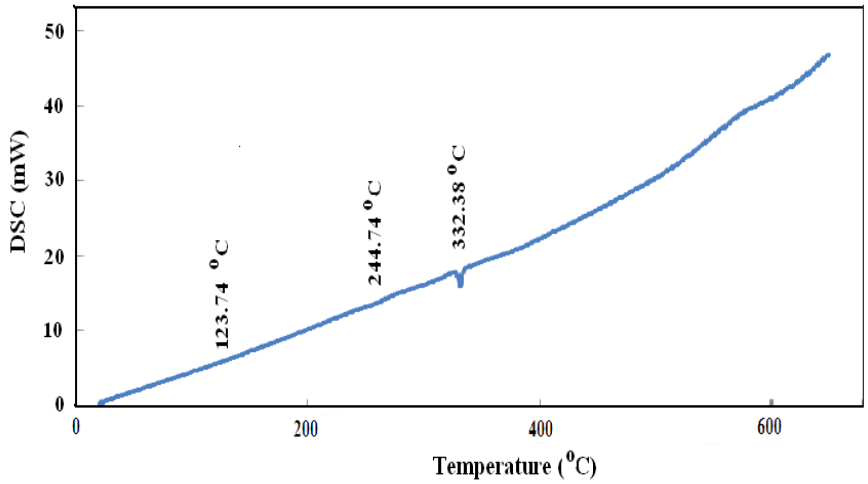

Fig. 2. DSC curve of the prepared lead oxide nano-particles

The obtained TGA and DSC data demonstrate that our prepared PbO nano-sized particles are more stable than the others prepared samples from lead oxalate. This could be due to the high calcination temperature during the preparation.

Fig. 3 illustrates the XRD pattern of the prepared PbO nano-powder. It is clear from the figure that, diffraction peaks were perfectly indexed to PbO, and nearly no impurity peak was observed [16,31]. This implies that the obtained product was good PbO consisting of a mixture of α- and β-PbO. The diffraction peaks were assigned to the orthorhombic β-PbO and the tetragonal α-PbO according to the peak positions (JCPDS card file No. 38-1477 and JCPDS card file No. 85-1739, respectively). The obtained data are in good agreement with those previously reported in earlier studies [7,16,32,33,34]. The primary phase in the present prepared powder was β-PbO. This could be attributed to the fact that the annealing temperature was above 400°C during the synthesis process. The organic acid employed for the gasification process has no effect on the obtained lead oxide structure. Sharp and intense peaks indicate excellent crystallization of the product. Several peaks of the corresponding β-PbO have not been marked with h k l values.

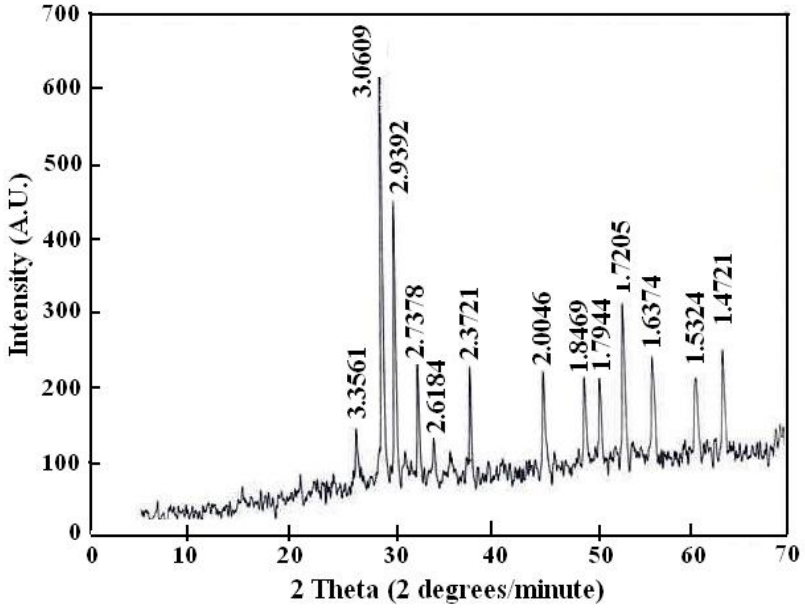

Fig. 3. XRD patterns of the obtained PbO nano-crystals

The crystalline size (D) of the PbO product was calculated using Scherrer's equation [16,31,35,36]:

$$D = 0.9\lambda/\beta \cos\theta \quad (1)$$

Where λ = 1.54056 Å, β is the full width at half maximum intensity (FWHM) and θ is the diffraction angle in degrees. It is notice from Table 1 that, the crystalline size of PbO ranged from 30.0 to 137.5 nm with an average crystalline size (D_{av}) in the range of 83.944 ± 28.679 nm. This value was calculated by using the equation [28]:

$$D_{av} = \Sigma D/n \quad (2)$$

where n is the number of the diffraction peaks corresponding to the 2θ values is 18. The calculated average crystalline size (D_{av}) is in good agreement with the value reported previously [28,31].

The strain induced in the obtained PbO nano-powders due to crystal imperfection and distortion was calculated using the relation [37]:

$$\varepsilon = \beta/4 \tan\theta \quad (3)$$

By plotting the values of β (in rad) against 4 tan θ gives a straight line relation with correlation coefficient (r) = 0.988 (Fig. 4). The slope of this straight line gives directly the strain (ε) value (≈ 8.685 x 10^{-3}) of the PbO nano-particles (by applying the least square fit to the experimental points). This indicates that the as-prepared PbO nano-particles have less imperfection. This strain confirms the specimen uniformity in all crystallographic directions, thus considering the isotropic nature of the crystal.

It is noteworthy to mention that the average crystalline size deduced from XRD data is well consistent with that observed by high-resolution transmission electron microscopy (HRTEM) and selective area electron diffraction (SAED). The SEM images of the as-prepared PbO nano-powders is observed in Figs. 5a, b. The SEM image showed that the particles morphology was disordered and that the particles were agglomerated. The agglomeration of the metal oxide in nano-range was due to the fact that it is hard to separate them into smaller single molecules, which is in a good agreement with those reported in earlier studies [16]. From the images, a broad distribution of the particle size was observed. The morphology of the obtained PbO powders with sol-gel method is uniform and smaller than 10 nm, consequently the particles are nano-sized. Fig. 5c shows the SAED pattern of the as-prepared PbO nano-powders. The pattern gives clear diffraction rings composed of spots suggesting that the as-prepared PbO nano-powders is single crystal with average crystal lattice shape of 6.371 nm [38]. HRTEM images of the as-prepared PbO nano-particles

were taken to investigate their average size and shape as shown in images 5d-f (Fig. 5). The images indicate that the PbO powder consists of nanometric particles with diameters ranging from 20 to 162 nm with an average particle size of 82.294 nm, which is consistent with the results of XRD.

Distinct lattice fringes could be seen in the HRTEM image of the as-prepared PbO. It is clear that the average lattice distance was measured to be 0.31 nm (Fig. 6). Those crystal arrangements showed that the crystal size is 0.31 nm, which is in agreement with the domain peak of XRD (0.306 nm). Therefore, the two results imply that the range of the sample is identical with the examination of the two techniques [38]. The average lattice distance measured for the sample is 0.31 nm, which are close to interplanar spacing between (101) crystal facets of β-PbO and confirms the formation of nanostructure.

Table 1. XRD data and particle size of the sol-gel synthesized PbO

No.	2θ (degree)	d-spacing (Å)	(hkl) [Refs. 2,14]	I/I_o	D (nm)
1	15.084	5.8687		2.5610	66.20
2	26.538	3.3561		2.5254	35.6
3	28.691	3.1089	(111) α	2.5568	137.5
4	29.152	3.0609	(101) β	2.5500	108.7
5	30.387	2.9392	(020) β	2.5518	119.5
6	31.324	2.8534		2.5630	104.8
7	31.868	2.8059	(110) α	2.5540	89.3
8	32.682	2.7378	(200) β	2.5514	111.3
9	34.217	2.6184		2.5615	53.9
10	37.900	2.3721	(201) β	2.5470	30.0
11	45.196	2.0046	(200) β	2.5490	121.7
12	46.270	1.9606	(200) α	2.5609	62.3
13	49.300	1.8469	(221) α	2.5546	66.3
14	50.845	1.7944	(202) β	6.7030	71.6
15	53.195	1.7205	(211) β	2.5510	87.0
16	56.128	1.6374	(311) β	2.5526	82.3
17	60.353	1.5324	(133) α	2.5353	82.5
18	63.102	1.4721	(040) β	2.2552	80.5

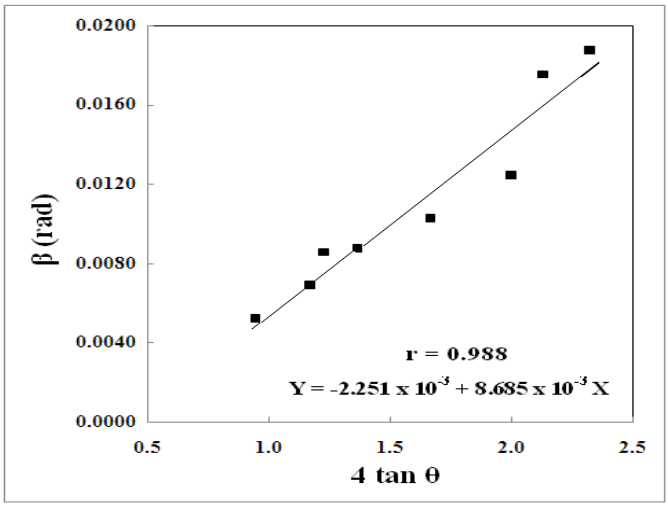

Fig. 4. Plot of the full width at half maximum (β) with 4 tan θ of the obtained PbO nano-crystals

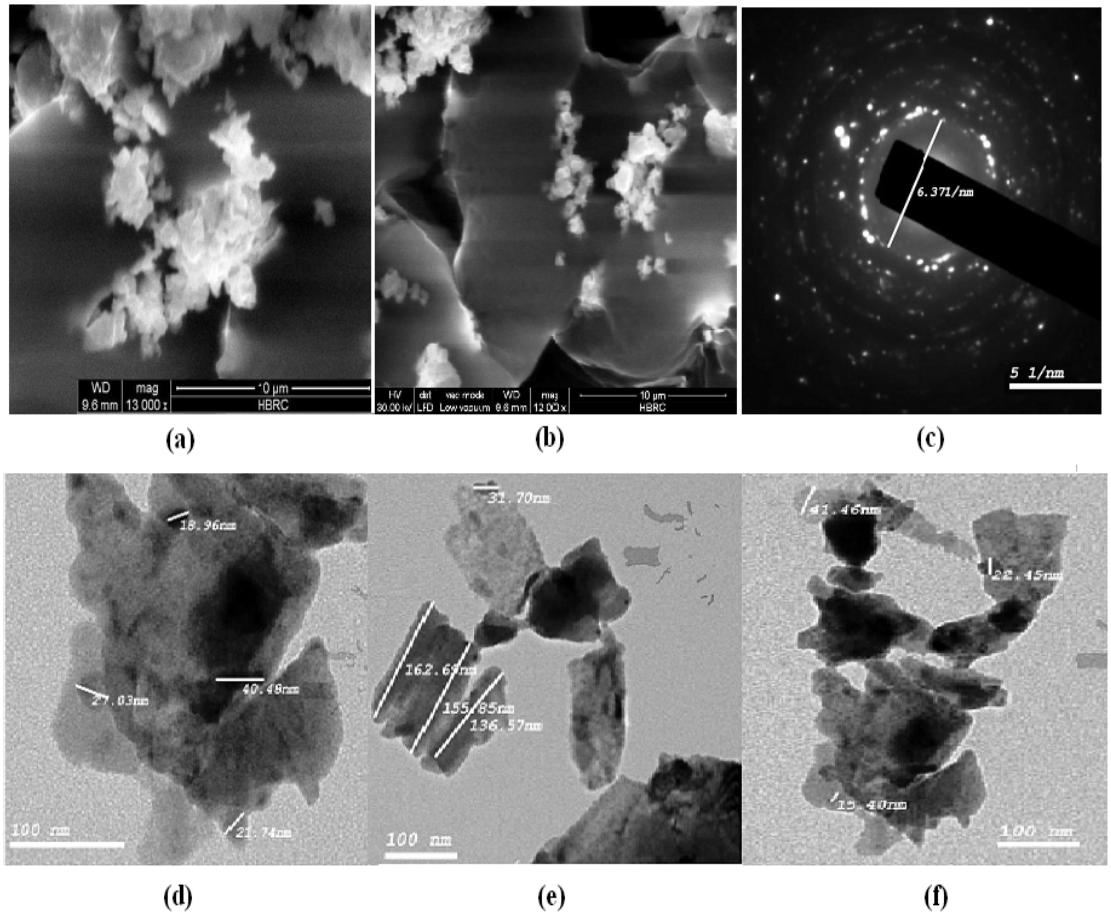

Fig. 5. (a, b) SEM images, (c) SAED pattern and (d, e, f) TEM images of PbO nano-crystals

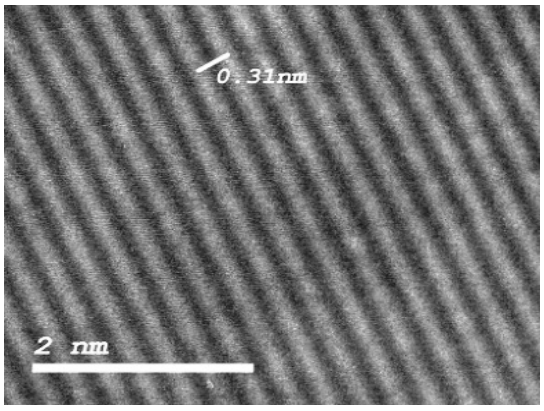

Fig. 6. HRTEM of PbO nano-crystals

FT-IR spectroscopy is a useful tool to help understand the functional group behavior of any organic molecule. The infrared spectra of the dry gel before drying (a) and drying powders at 400°C for 2 hours (b), were shown in Fig. 7. As shown in Fig. 7a, the broad absorption band around 3441 cm^{-1} corresponds to the v_{O-H} stretching vibrations of water molecules [2,30]. Two absorption bands at about 2919 and 2855 cm^{-1} were attributed to the asymmetric CH_2 stretch and the symmetric CH_2 stretch, respectively [39]. The absorption band that appears at around 1632 cm^{-1} is due to the asymmetric vibrations of the carbonyl group [16]. The absorption band at about 1400 cm^{-1} is due to the v_S(C-O) and v_δ(OC=O) vibrational modes. The band at about 845 cm^{-1} corresponds to CH_2 rocking vibration mode. Bending mode of the phenyl group, v (benzene ring), at around 695 and 683 cm^{-1} were detected. The absorption band at about 500 cm^{-1} was attributed to Pb–O bond [2,16]. In the FT-IR spectrum of the PbO nano-powders (Fig. 7b); after drying at 400°C for 2 hours, a new peak appears at about 450 cm^{-1}, which is assigned to the Pb–O bond.

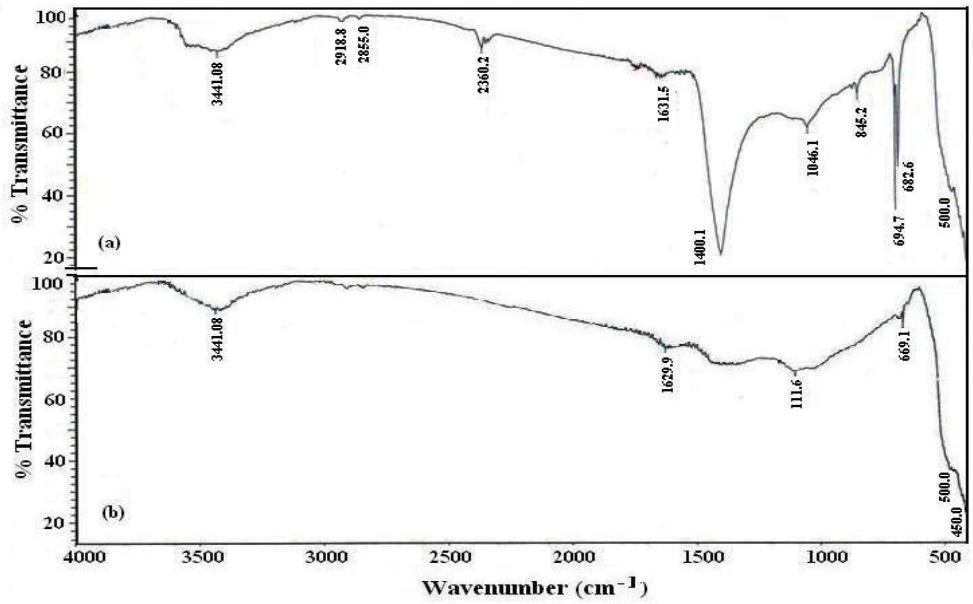

Fig. 7. FT-IR spectra of PbO nano-powders (a) Before drying and (b) After drying at 400°C for 2 hours

4. CONCLUSIONS

In summary, we have performed the synthesis of PbO nano-crytallites via sol–gel method. This method is simple, inexpensive, and economical and was introduced as reproducible process for the large-scale synthesis of PbO nano-particles. The XRD analysis indicates that the obtained PbO was a mixture of two phases; the orthorhombic β-PbO and the tetragonal α-PbO. The prepared PbO powder consists of crystallites of about 84 nm. The morphology of the obtained PbO powders with sol-gel method is uniform and smaller than 10 μm, so, the particle will be expected to be in nano-size. The SAED pattern indicates that the as-prepared PbO nano-powder is single crystal. HRTEM images of the PbO nano-particles indicate that the PbO powder consists of nanometric size. The average particle size (about 82 nm) is consistent with the results of XRD.

COMPETING INTERESTS

Authors have declared that no competing interests exist.

REFERENCES

1. Ranjbar ZR, Morsali A. Sonochemical syntheses of a new nano-sized porous lead(II) coordination polymer as precursor for preparation of lead (II) oxide nanoparticles. J. Mol. Struct. 2009;936: 206–12.
2. Salavati-Niasari M, Mohandes F, Davar F. Preparation of PbO nanocrystals via decomposition of lead oxalate. Polyhedron. 2009;28:2263–7.
3. Ferg EE, Phangalala T, Dyl T. A new look at determining acid absorption of lead oxide used in the manufacturing of Pb-acid batteries. J. Appl. Electrochem. 2010;40: 383-91.
4. Liu S, Tang ZR, Sun Y, Colmenares JC, Xu YJ. One-dimension-based spatially ordered architectures for solar energy conversion. Chem. Soc. Rev. 2015;44: 5053-75.
5. Nandy P, Bandyopadhyaya P, Deya A, Basu R, Das S. Synthesis and characterization of copper doped zinc oxide nanoparticles and its application in energy conversion. Current Applied Physics. 2014;14:1149-55.
6. Li S, Yang W, Chen M, Gao J, Kang J, Qi Y. Preparation of PbO nanoparticles by microwave irradiation and their application to Pb(II)-selective electrode based on cellulose acetate. Mater. Chem. Phys. 2005;90:262-9.
7. Karami H, Karami MA, Haghdar S. Synthesis of uniform nanostructured lead oxide by sonochemical method and its

application as cathode and anode of lead-acid batteries. Mater. Res. Bull. 2008;43:3054-65.

8. Karami H, Karami MA, Haghdar S, Sadeghi A, Mir-Ghasemi R, Mahdi-Khani S. Synthesis of lead oxide nanoparticles by Sonochemical method and its application as cathode and anode of lead-acid batteries. Mater. Chem. Phys. 2008;108: 337-44.
9. Zhang L, Guo F, Liu X, Cui J, Qian Y. Metastable PbO crystal grown through alcohol-thermal process. J. Cryst. Growth. 2005;280:575-80.
10. Lu BT, Luo JL, Lu YC. Effects of pH on lead-induced passivity degradation of nuclear steam generator tubing alloy in high temperature crevice chemistries. J. Nucl. Mater. 2012;429:305-14.
11. Kumaravel R, Krishnakumar V, Ramamurthi K, Elamurugu E, Thirumavalavan M. Deposition of $(CdO)_{1-x}(PbO)_x$ thin films by spray pyrolysis technique and their characterization. Thin Solid Films. 2007;515:4061-5.
12. Perry DL, Wilkinson TJ. Synthesis of high-purity α- and β-PbO and possible applications to synthesis and processing of other lead oxide materials. Appl. Phys. A. 2007;89:77–80.
13. Li L, Zhu X, Yang D, Gao L, Liu J, Kumar RV, Yang J. Preparation and characterization of nano-structured lead oxide from spent lead acid battery paste. J. Hazard. Mater. 2012;203:274-82.
14. Xi G, Peng Y, Xu L, Zhang M, Yu W, Qian Y. Selected-control synthesis of PbO_2 submicrometer-sized hollow spheres and Pb_3O_4 microtubes. Inorg, Chem. Commun. 2004;7:607-10.
15. Lafronta AM, Zhanga W, Ghalia E, Houlachib G. Electrochemical noise studies of the corrosion behaviour of lead anodes during zinc electro-winning maintenance. Electrochem. Acta. 2010;55: 6665-75.
16. Kashani-Motlagh MM, Mahmoudabad MK. Synthesis and characterization of lead oxide nano-powders by sol-gel method. J. Sol-Gel Sci. Techn. 2011;59:106–10.
17. Geckeler KE, Nishide H. Advanced nanomaterial. Wiley-VCH Verlag GmbH & Co. KGaA, Weinheim; 2011.
18. Pan ZW, Dai ZR, Wang ZL. Lead oxide nanobelts and phase transformation induced by electron beam irradiation. Appl. Phys. Lett. 2002;14:309-11.
19. Jiang XC, Wang YL, Herricks T, Xia Y. Ethylene glycol-mediated synthesis of metal oxide nanowires. J. Mater. Chem. 2004;14:695-703.
20. Juan CL, Mao ZS, Shen WZ, Jun ZZ, Xin DH. Preparation of PbS-type PbO nanocrystals in a room-temperature ionic liquid. Mater. Lett. 2005;59:3119-21.
21. Jia B, Gao L. Synthesis and characterization of single crystalline PbO nanorods via a facile hydro-thermal method. Mater. Chem. Phys. 2006;100: 351-4.
22. El-Sayed Abdo A, Ali MAM, Ismail MR. Natural fibre high-density polyethylene and lead oxide composites for radiation shielding. Radiat. Phys. Chem. 2003;66: 185-95.
23. Zhong WH, Sui G, Jana S, Miller J. Cosmic radiation shielding tests for UHMWPE fiber/nano-epoxy composites. Compos. Sci. Technol. 2009;69:2093-7.
24. Erdem M, Baykara O, Dogru M, Kuluozturk F. A novel shielding material prepared from solid waste containing lead for gamma ray. Radiat. Phys. Chem. 2010;79:917-22.
25. Harish V, Nagauah N, Prabhu TN, Varughese KT. Thermo-mechanical analysis of lead monoxide filled unsaturated polyester based polymer composite radiation shields. J. Appl. Polym. Sci. 2010;117:3623-9.
26. Uhm YR, Kim J, Lee S, Jeon J, Rhee CK. In situ fabrication of surface modified lead monoxide nanopowder and its HDPE nanocomposite. Ind. Eng. Chem. Res. 2011;50:4478-83.
27. Hassen A, El Sayed AM, Morsi WM, El-Sayed S. Influence of Cr2O3 nanoparticles on the physical properties of polyvinyl alcohol. J. Appl. Phys. 2012;112:093525.
28. El Sayed AM, Morsi WM. Dielectric relaxation and optical properties of polyvinyl chloride\lead monoxide nanocomposites. Polym. Composite. 2013; 34:1977–2168.
29. Sankar V, Suresh Kumar T, Panduranga Rao K. Preparation, characterization and fabrication of intraocular lens from photo initiated polymerized poly(methyl methacrylate). Trends Biomater. Artif. Organs. 2004;17:24-30.
30. Sadeghzadeh H, Morsali A, Yilmaz VT, Büyükgüngör O. Synthesis of PbO nano-particles from a new one-dimensional lead (II) coordination polymer precursor. Mater. Lett. 2010;64:810–3.

31. Mahmoudabad MK, Kashani-Motlagh MM. Synthesis and characterization of PbO nanostructure and NiO doped with PbO through combustion of citrate/nitrate gel. Int. J. Phys. Sci. 2011;6:5720-5.
32. Wilkinson TJ, Dale L. Perry DL, Spiller E, Berdahl P, Derenzo BP, Weber MJ. A facile wet synthesis of nanoparticles of litharge, the tetragonal form of PbO. Proceed. Mater. Res. Soc. 2002;704: 117-22.
33. Hashemi L, Morsali A. Synthesis and characterization of a new nano lead (II) two-dimensional coordination polymer by sonochemical method: A precursor to produce pure phase nano-sized lead (II) oxide. J. Inorg. Organomet. Polym. 2010; 20:856–61.
34. Safarifard V, Morsali A. Sonochemical syntheses of nano lead(II) iodide triazole carboxylate coordination polymer: Precursor for facile fabrication of lead(II) oxide/iodide nano-structures. Inorg. Chim. Acta. 2013;398:151-7.
35. Scherrer P. Bestimmung der grobe und der inneren struktur von kolloidteilchen mittels rontgenstrahlen. Nachrichten von der Gesellschaft der Wissenschaften zu Gottingen. 1918;2:98-100.
36. Eshaghi A, Pakshir M, Mozaffarinia R. Preparation and characterization of TiO_2 sol-gel modified nanocomposite films. J. Sol- Gel Sci. Technol. 2010;55:278-84.
37. Mote VD, Purushotham Y, Dole BN. Wlliamson-Hall analysis in estimation of lattice strain in nanometer-sized ZnO particles. Journal of Theoretical and Applied Physics. 2012;6, article 6.
38. Chen KC, Wang CW, Lee YI, Liu HG. Nanoplates and nanostars of β-PbO formed at the air/water interface. Colloids and Surfaces A: Physicochem Eng Aspects. 2011;373:124–9.
39. Yang HT, Shen CM, Wang YG, Su YK, Yang TZ, Gao HJ. Stable cobalt nanoparticles passivated with oleic acid and triphenylphosphine. Nanotechnology. 2004;15:70-4.

Peer-review history:
The peer review history for this paper can be accessed here:
http://sciencedomain.org/review-history/15586